Light-Driven Molecular Whirligig

Chuan Gao, Andreas Vargas Jentzsch, Emilie Moulin, Nicolas Giuseppone

A light-driven molecular whirligig

Chuan Gao,[a] Andreas Vargas Jentzsch,[a] Emilie Moulin[a] and Nicolas Giuseppone*[a]

[a] SAMS Research Group, Université de Strasbourg, CNRS, Institut Charles Sadron UPR22, 67000 Strasbourg, France

ABSTRACT: An unidirectional light-driven rotary motor was looped in a figure-of-eight molecule by linking two polymer chains between its stator and rotor parts. By properly tuning the size of these linkers, clockwise rotation of the motor under UV light was shown to create conformationally strained twists between the polymer chains and, in this tensed conformation, the energy stored in the molecular object was sufficient to trigger the reverse rotation of the motor back to its fully relaxed state. The functioning principle of this motorized molecular device appears very similar to the one of macroscopic whirligig crafts used by children for fun. In addition, we found that in its out-of-equilibrium tensed state, the fluorescence emission of the molecular motor increased by 500% due to the mechanical constraints imposed by the polymer chains on its conjugated core. Finally, by calculating the apparent thermal energies of activation for the backward rotations at different levels of twisting, we quantitatively determined a lower estimate of the work generated by this rotary motor, from which a torque and a force were extracted, thus answering a long-term open question in this field of research.

INTRODUCTION

Synthetic chemists working in the field of artificial molecular machines[1–9] often take inspiration from machines that we know and use at macroscale (elevators,[10,11] cars,[12,13] pumps[14–16] and transporters,[17,18] robots and synthesizers,[19,20] muscles,[21–24] walkers,[25,26] etc). Even if the functioning principles are different at nanoscale because of the Brownian environment,[27–30] it appears very fruitful to make use of such analogies with the macroscopic scale to potentially find new ideas and useful applications.[31–33] Toward this direction, there is also an imperative need to interface these nanomachines with their environment and integrate them at all scales in order to make use of their motions[34–36] as well as to convert, store, and release energy.[37,38]

In the present work, our macroscopic inspiration came from the whirligig crafts used by children for fun (Figure 1a). In this very simple toy, the forward rotation of a circular disc results in the twisting of the strings passing through its center, and leading to an accumulation of elastic energy by the whirligig craft. In such a tensed conformation, the backward rotation of the disc can be activated by the torque generated from the twists, leading to the unwinding of the strings through the release of their elastic energy. When increasing the power applied by pulling on the strings, the system can produce faster alternation of clockwise and anticlockwise rotations.[39] To achieve a similar principle at the molecular scale, and therefore without the help of inertia, we based our strategy on the figure-of-eight molecule **W3** we originally designed back in 2015 (Figure 2a).[40] This molecule combines a second generation light-driven rotary motor with two polymer chains creating two loops between its rotor and stator parts. We already studied and proved the internal twisting of the polymer chains by activation of the clockwise motor rotation using AFM and SAXS measurements. It should be noted that a variation of our early figure of eight appeared very recently in a publication by Feringa *et al*.[41] In this highly interesting study, the authors integrated 2 exchangeable imine bonds in the polymer loops and, by twisting the system, they demonstrated the subsequent impact on the out-of-equilibrium population of the different possible twisted imines, as compared with the distribution at thermodynamic equilibrium. With our original figure-of-eight construct, that is with no possible chemical exchange through dynamic covalent bonds, we wanted to study the possibility to make the rotation of the system reversible by clockwise and anticlockwise rotations at the motor level (Figure 1b). In particular, in an analogy with the whirligig craft, we wanted to probe the potential anticlockwise rotation of the motor through the ground state helped by the mechanical tension created within the twisted conformation. Hereafter, we demonstrate that indeed rotation of the molecular motor can be fully reversed by the strained twists generated by its initial rotation. We also highlight how this out-of-equilibrium situation can be coupled to a strong enhancement of the motor fluorescence which subsequently decreases when the system dissipates strains. Finally, we quantitatively determine important characteristics of this machine, such as the mechanical work produced, the value of the torque, and the force generated.

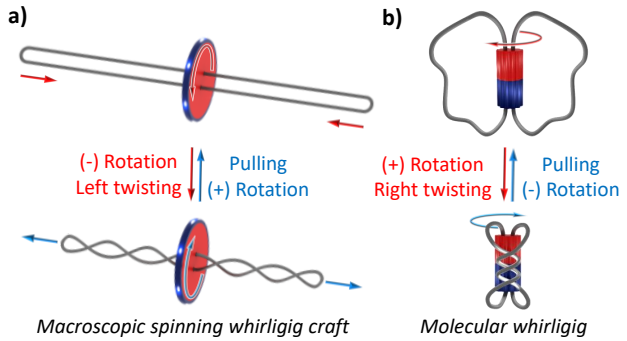

Figure 1. Schematic representation of a macroscopic spinning whirligig craft **(a)** and of a molecular whirligig as designed in the present study, and which involves a light-driven rotary motor entangled in a figure of 8 using polymer chains **(b)**. In both cases, at macro and nanoscale, the rotation of the central unit involves a twisting of the strings attached, and the untwisting of these strings enforces the back rotation of the central unit.

RESULTS AND DISCUSSION

This work started with the synthesis of molecular whirligigs **W1**, **W2**, and **W3** incorporating the same central second-generation light-driven rotary motor, but with different lengths of polyethyleneglycol (PEG) chains to loop the upper and lower part of the motor in the figure of eight (Figure 2a). The idea behind the variation of the chain lengths was to change the possible number of twists generated by the motor rotation, as well as the resulting mechanical tension to reverse the rotation. Using our previously described bis-acid bis-alkyne motor **2**,[40] we performed classical amidation reactions, in the presence of EDC and HOBt, with NH_2-PEG_5-N_3 ($M_w \approx 300$ g.mol^{-1}), NH_2-PEG_{73}-N_3 ($M_w \approx 3000$ g.mol^{-1}), and NH_2-PEG_{248}-N_3 ($M_w \approx 10000$ g.mol^{-1}). Star-shaped molecular motors **S1**, **S2**, and **S3** were respectively obtained with yields comprised between 52% and 90% (see SI for detailed synthetic protocols and characterizations, sections S1 and S8). Molecular whirligigs **W1**, **W2**, and **W3** were then synthesized with yields comprised between 43% and 71% by intramolecular cyclisation using copper-catalyzed azide–alkyne cycloaddition (CuAAC) reactions from diluted DMF solutions (c = 0.5–1 10^{-4} M). The structures and purity of the three molecules were unambiguously confirmed by NMR spectroscopies and mass spectrometry (see SI).

Starting with **W1**, we probed the possibility to wind its polymer chains under UV irradiation through the rotation of the motor. As represented in Figure 2b, each 180° clockwise rotation of the motor should create a supplementary crossing of the polymer chains leading to right handed twists. In the following, the number **X** of half-rotations / crossings compared to the initial molecule **W1** will be denoted as **W1-X**.[42,43] An important asset of **W1** is that it exists as a single (monodisperse) molecule, and not as a polymeric structure with a distribution of molecular weights such as it is the case for **W2** and **W3**. Very satisfyingly, this property allowed us to accurately follow the evolution of its conformation upon light irradiation using ultra performant liquid chromatography coupled to mass spectrometry (UPLC-MS) (Figure 3a). Initially, **W1** was solubilized in THF (c = 230 µM) at a temperature of 293 K in the dark. The corresponding chromatogram confirmed the presence of a single species with an elution time at 1.77 min and displaying the expected mass spectrum of **W1** (Figure 3a,b). Interestingly, UV irradiation of the **W1** solution (365 nm, 1.2 mW.cm^{-2}) for 35 min led to the appearance of new species perfectly separated on the UV-Vis chromatograms. Because the mass spectra of all the new appearing peaks remain superimposable (Figure 3b and S1), we were reinforced in our expectations that these isomers were obtained by the repetitive 180° clockwise rotation of the motor, leading first to **W1-1** (elution time 1.73 min), then **W1-2** (retention time 1.91 min), and then **W1-3** (retention time 2.08 min). The full distribution profile of this irradiation experiment is plotted in Figure 3c, which illustrates better the relationship between the species. From 5 min to 30 min, the ratio **W1-1**/**W1-2** gradually decreased over time and **W1-2** became the main component. It reveals that **W1** first transformed to **W1-1**, which subsequently converted to **W1-2**. Moreover, from 30 min to 35 min, the percentage of **W1-1** remained unchanged and the ratio of **W1-2**/**W1-3** decreased, indicating the transformation from **W1-2** to **W1-3**. After 35 min of irradiation, the system reached the photo-stationary state (PSS). According to these results, the transformation of **W1** under light irradiation can be clearly established, that is **W1** → **W1-1** → **W1-2** → **W1-3**. It should be noted that in the described experimental conditions, no degradation was observed over the full experiment, but attempts to increase the lamp power led to new products with mass spectra different from the necessarily invariable **W1-X** figure of eight.

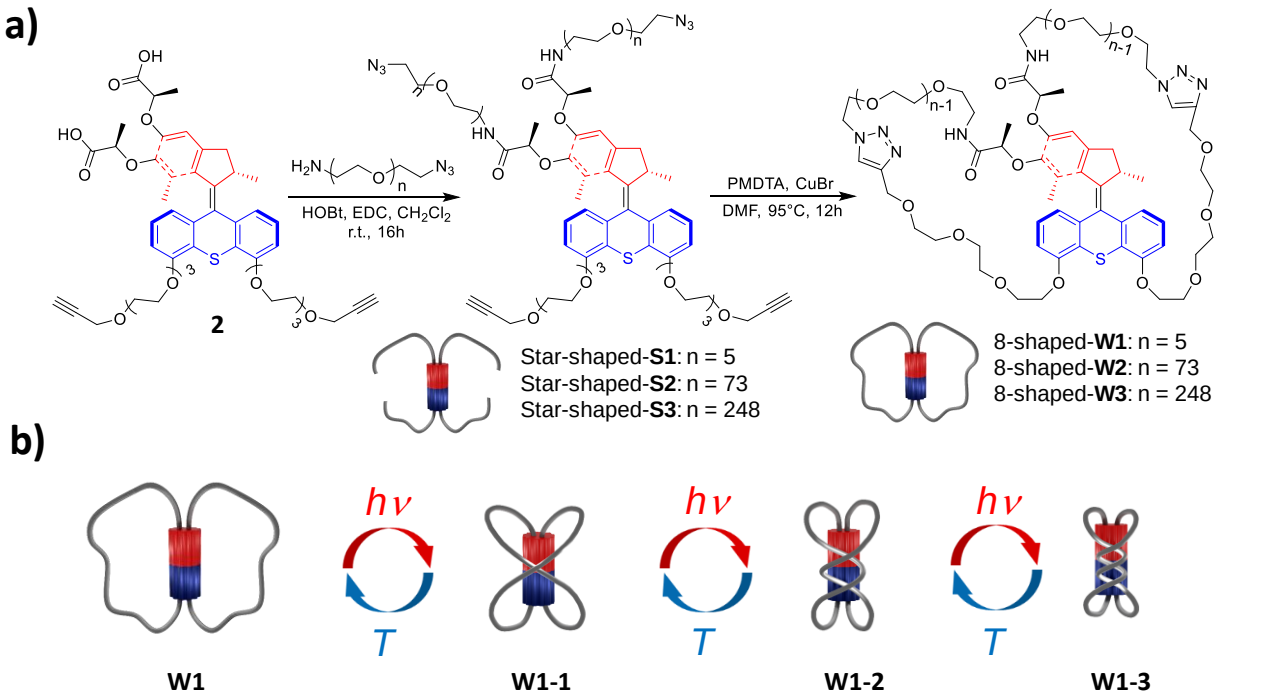

Figure 2. (a) Synthetic pathway for molecular whirligigs **W1**, **W2**, and **W3**, from motor **2**, incorporating different lengths of polyethylene glycol chains. **(b)** Schematic representation of the forward and backward stepwise 180° rotations of molecular whirligig **W1**, leading to new entanglements in the figure of eight and incorporating 1, 2, or 3 crossings (**W1-1**, **W1-2**, and **W1-3**, respectively).

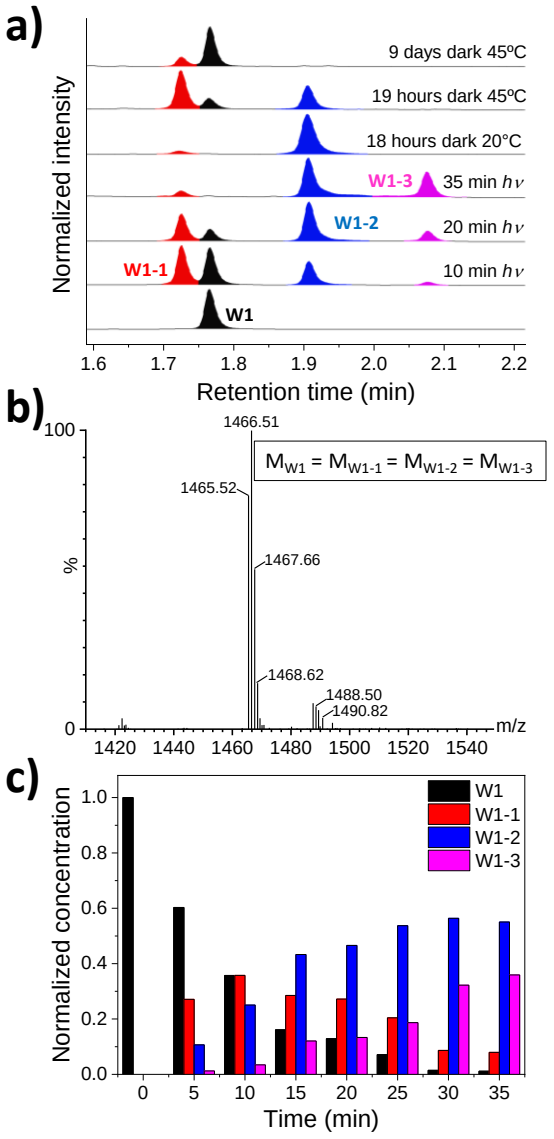

Figure 3. (a) UPLC-MS/UV chromatograms of molecular whirligig **W1** in THF (230 µM) for different times of light irradiation (365 nm, 1.2 mW.cm^{-2}), and subsequent heating in the dark. **(b)** Typical mass spectrum displayed by all isomers **W1**, **W1-1**, **W1-2**, and **W1-3** after UPLC separation. **(c)** Normalized concentrations of twisted isomers as a function of irradiation times.

After this irradiation sequence, we subsequently let the system evolve at the same temperature in the dark, and followed its evolution using the same UPLC-MS protocol (Figure 3a). After 18 hours at 20 °C, **W1-3** fully transformed to **W1-2**. Because the next steps were slow at 20 °C, the temperature was then raised to 45 °C to collect the necessary information within a reasonable period of time. Interestingly, **W1-2** was gradually transformed into **W1-1**, which further converted to **W1**. After 9 days, the system reached the thermodynamic equilibrium. The order of disappearance of the 4 isomers is symmetric to their appearance under light irradiation. In this particular construct, the only possibility for the system to go back to **W1** from its twisted isomers is to do it by inversion of the motor rotation (that is here anticlockwise) and by crossing both thermal helix inversion and *E*/*Z* isomerization by the ground state.

Before analyzing in more details the kinetic data corresponding to these UPLC traces, we performed a few 1D and 2D ^{1}H NMR experiments to confirm the global evolution of the system (Figure 4). Large chemical shifts were observed for a number of resonance signals in ^{1}H NMR spectra starting from **W1** under photoexcitation (365 nm, 1.2 mW.cm^{-2}) (Figure 4a,d). Here, because of the higher concentration of the sample compared to UPLC experiments, longer irradiation times were necessary (up to 510 min to reach the PSS). In particular, the triazol protons (k,l) were particularly affected by the rotation of the motor, leading to new signals shifted both downfield and upfield. On the motor part, protons j, p, q, and v were also particularly affected. Satisfyingly, the relaxation in the dark proved the full reversibility of the process, in agreement with UPLC-MS experiments, and with an almost full recovery of **W1** at thermodynamic equilibrium (in addition to minor amounts of **W1-1**) (Figure 4e). NOESY NMR spectra were also recorded between the initial state containing pure **W1**, and after 510 min of UV irradiation containing mostly twisted compounds **W1-2** and **W1-3** (Figures 4b,c, S4 and S6). The appearance of new spatial correlations upon light irradiation, in particular those showing the closer proximity between the central motor and the polymer chains are in good agreement with our initial claim of the induced twisting upon rotation.

At that stage of the study, we noticed by naked eye an increase of the fluorescent emission of the whirligig solutions with irradiation time, and we decided to determine the origin of this phenomenon. In this direction, we first performed a series of experiments by UV-Vis and electronic circular dichroism (CD) spectroscopies. Upon UV irradiation (365 nm, 1.2 mW.m^{-2}), the absorption intensity of **W1** between 322 and 400 nm decreased very slightly, with a PSS reached after 25 min. Moreover, the absorption peak slightly shifted from 330 nm to 322 nm, in agreement with a more tensed conformation. After 18 hours in the dark at 20 °C, the UV spectrum slightly evolved in the opposite direction, as expected for the transformation of **W1-3** in **W1-2** (Figure 5a). Although these changes are very subtle, they are real and significant. Indeed, the same experiment performed on open molecule **S1** as reference did not produce any measurable change (Figure S7). To further investigate the conformational change of **W1**, we performed CD experiments on the same solutions. As shown in Figure 5b, the CD spectrum showed no noticeable change and, in particular, no signal inversion, indicating that the unstable helix of the motor was not 'trapped' after rotation in the twisted forms. As observed with UV-Vis, the transformation of **W1-3** in **W1-2** led to the slight reversibility of the CD signal (Figure 5b).

We then turned to fluorescence spectroscopy upon twisting of **W1** at 365 nm, and measured a gradual increase of emission intensity from 469 nm to 461 nm that reached 500% at the PSS (Figure 5c). The similar shapes of the spectra suggest a mechanical restriction of the movement as a possible origin of the enhancement in fluorescence. Therefore, in parallel, we studied the fluorescence emission of a reference motor **M1** in solution and evidenced an important aggregation induced emission (AIE) with an enhanced emission from 465 nm to 458 nm following the addition of increasing amounts of water in THF (Figure S8).[44–46] Therefore, the enhancement of fluorescence intensity within the whirligig device is certainly the consequence of the limitation of intramolecular motions in **W1** by increasing the conformational strain induced by the twisting of the PEG chains upon rotation. Back transformation from **W1-3** to **W1-2** in the dark led to a drop of emission intensity by 40% because of the release of conformational strain (Figure 5c, dash line).

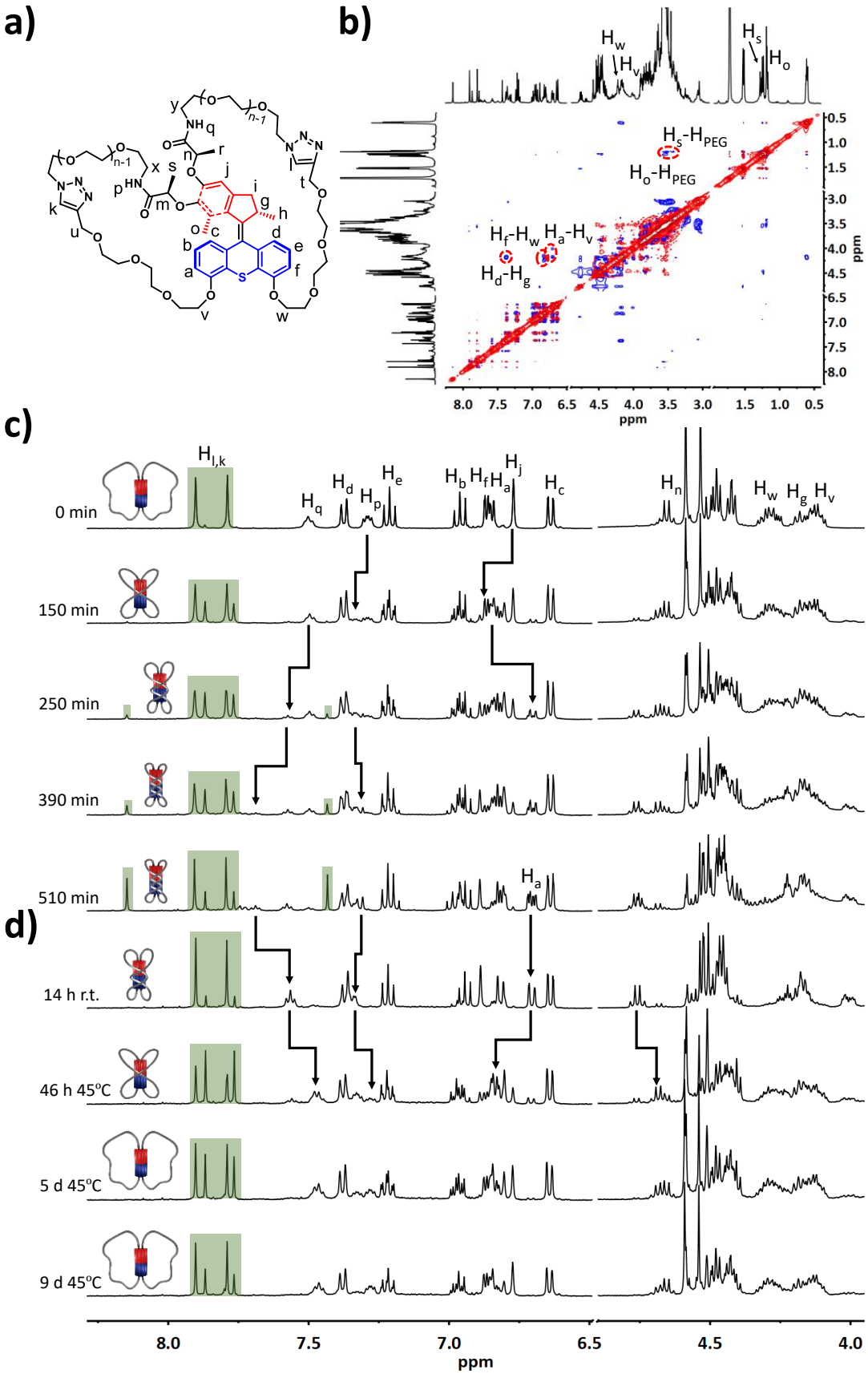

Figure 4. (a) Chemical structure of molecular whirligig **W1**. **(b)** 2D NOESY spectra of **W1** after 510 min of UV light irradiation (365 nm, 1.2 mW.cm^{-2}). **(c-d)** ^{1}H NMR spectra of **W1** (400 MHz, THF-d_8, 298 K, c = 10 mM) for different irradiation (**c**) and subsequent heating times (**d**).

Going further, we tried to correlate the 500% increase of fluorescence by measuring the relative quantum yields of the twisted species by pushing the system at the PSS (see SI, section S5). We found a value of 0.08% for **W1** and of 0.4% at the highest PSS (36% **W1-3**; 55% **W1-2**; 9% **W1** + **W1-1**). In addition, and as an overall correlation of the increased tension generated with the generation of new twists, we measured a significant decrease of the photo-isomerization quantum yields, from about 11% for **W1** to **W1-1** and **W1-1** to **W1-2**, to about 3% for the transformation **W1-2** to **W1-3** (see SI, section S6).

Interestingly, the plot of maximum emission intensity of **W1** as a function of irradiation time shows a clear sigmoid shape (Figure 5d). The first 7 min of irradiation (corresponding to the first 10 min of irradiation in UPLC due to a change in concentration (Figure 3)) induced a relatively slow emission enhancement. However, from 7 min to 22 min (corresponding to 10 min to 30 min in Figure 3) the emission intensity increased more rapidly due to the increase in the percentage of **W1-3** (Figure 3), and in agreement with a much higher conformational strain of **W1-3** compared to **W1-2**. Because the transformation from **W1-3** to **W1-2** can be reversed after 18 hours at 20 °C in the dark, we were pleased to also notice a decrease of fluorescence after this time (dashed line in Figure 5c). Satisfyingly, a subsequent irradiation of 6 min resulted in the full recovery of the emission spectrum of the tensed state **W1-3** (Figure 5e). This reversed transformations between **W1-3** to **W1-2** by opposite 180° rotations could be repeated for at least 3 irradiation/dark cycles (Figure 5f). This observed phenomenon is in itself remarkable as it confers a dissipative out-of-equilibrium tunable function to the system through an original motorized induced emission (MIE) and which is due to the mechanical restriction of the internal molecular motions of the fluorophore.

Then, we probed the behavior of **W2** and **W3** by the same optical measurements (Figures S9 and S10). In both cases, UV and CD spectra remained almost fully superimposable, revealing a smaller conformational impact of the rotation on the motor itself. In agreement, the fluorescence enhancement was limited to 100% for **W2** and to 50% for **W3** after reaching the PSS. Therefore, one can suggest that the tension created in the whirligig is inversely proportional to the length of the polymer chains. This interpretation is further reinforced by the fact that the system was much less reversible for longer polymer chains. Indeed, **W2** was shown to produce the same fluorescence intensity at the PSS and after 20 hours at 45 °C in the dark. In addition, in this case, gel permeation chromatography (GPC) allowed us to measure a decrease of the apparent mass of **W2** from $M_{w,app}$ = 6424 g.mol^{-1} before irradiation, to $M_{w,app}$ = 4592 g.mol^{-1} after irradiation, confirming by another technique the twisting of the polymer chains and the contraction of the molecule (Figure S11). However, in agreement with the fluorescence signal, we did not measure any clear untwisting of the system after 20 hours in the dark at 45°C ($M_{w,app}$ = 4714 g.mol^{-1}).

Overall, by combining chromatographic, spectroscopic and spectrometric methods, we can strongly validate the whirligig concept we propose in this paper, and restrict its validity to entangled systems which can produce highly strained conformations out-of-equilibrium, and which may be limited to relatively small polymer chains.

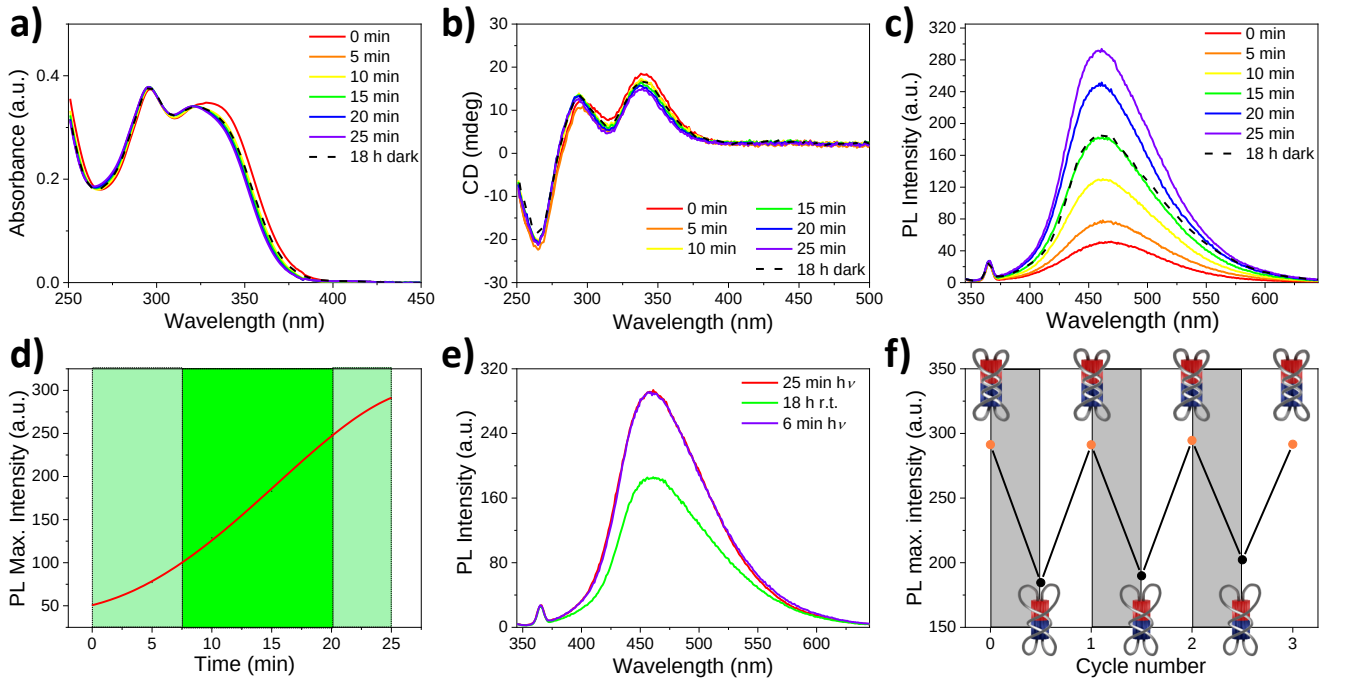

Figure 5. (a) UV-Vis spectra of **W1** (THF, 25 µM) for different irradiation times (solid line) and after 18 hours in the dark at 20 °C (dashed line); **(b)** CD spectra of **W1** (THF, 25 µM) for different irradiation times (solid line) and after 18 hours in the dark at 20 °C (dashed line); **(c)** Emission spectra of **W1** (THF, 25 µM) for different irradiation times (solid line) and after 18 hours in the dark at 20 °C (dashed line); **(d)** Maximum emission intensity of **W1** for different irradiation times; **(e)** Emission spectra of **W1** (THF, 25 µM) for an initial 25 min irradiation time (red solid line), after 18 hours in the dark at 20 °C (green line) and after re-irradiation for 6 min (purple solid line); **(f)** Out-of-equilibrium modulation of the maximum emission intensity during three irradiation/dark cycles as in **(e)**.

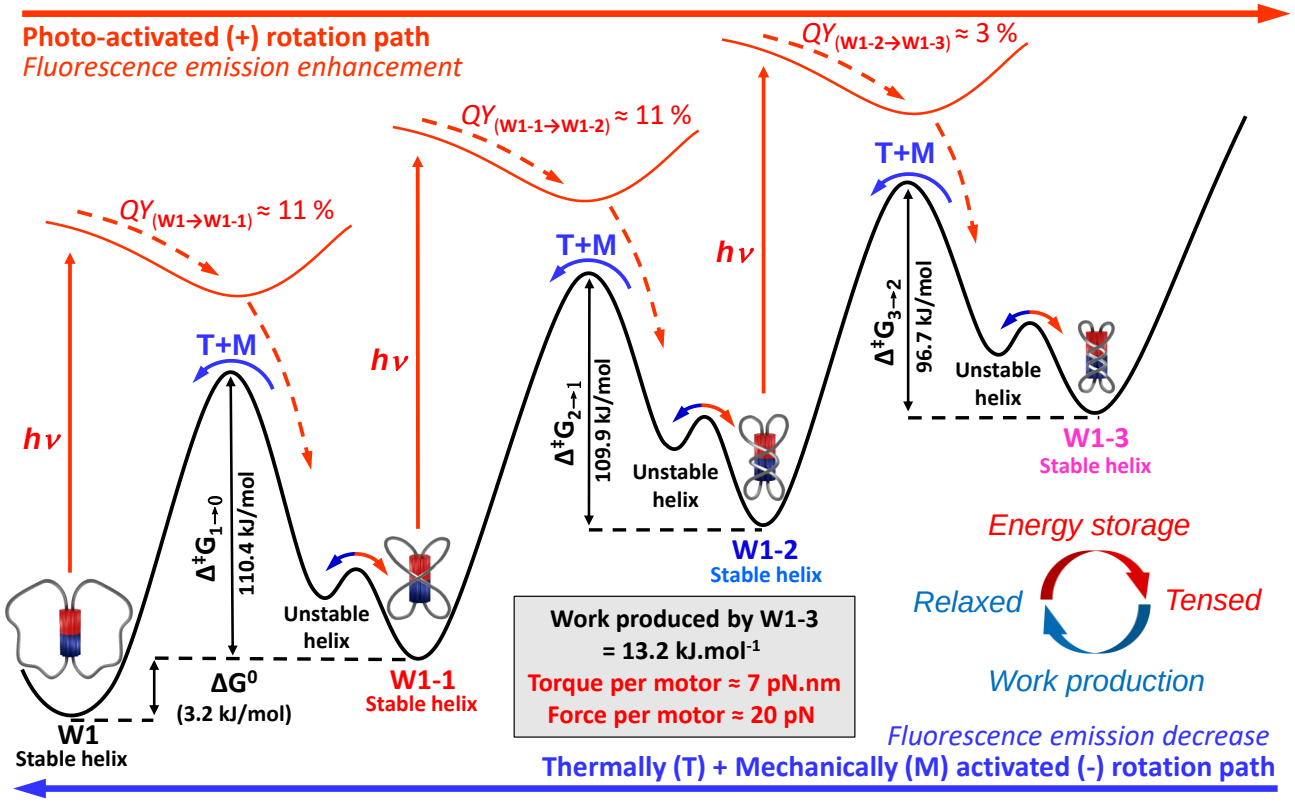

Figure 6. Energy diagram of molecular whirligig **W1**, involving a fully reversible 540° rotation. As the system is pushed out of equilibrium by light through the photoexcited state, it stores energy in the form of mechanical tension. This tension is then producing a work which is sufficient to enforce the back rotation of the motor through isomerizations at the ground state (helix inversion and *E*/*Z* isomerization). The gain in the apparent activation energy compared to the untwisted system is the result of the torque generated by the tensed whirligig.

To extract a quantitative mechanical information from our system using **W1**, we fitted the relaxation data obtained in the dark from UPLC-MS chromatograms at 4 different temperatures, and performed Eyring plot analyses for the three transformations **W1-3** to **W1-2**, **W1-2** to **W1-1**, and **W1-1** to **W1** (see SI section S6). We found that the apparent activation energies necessary to reverse the motor rotation at the ground state are the following: 110.4 kJ.mol^{-1} for **W1-1** (corresponding to a half-time of the anticlockwise rotation of 62 days at 20 °C); 109.9 kJ.mol^{-1} for **W1-2** (corresponding to a half-time of the anticlockwise rotation of 51 days at 20 °C) and 96.7 kJ.mol^{-1} for **W1-3** (corresponding to a half-time of the anticlockwise rotation of 5.7 hours at 20 °C). These activation energies encompass both thermal and mechanical contributions. Because we observed both **W1** and **W1-1** at thermodynamic equilibrium, we were also able to determine a reference activation energy (that is purely thermally activated) to isomerize the double bond of **W1** (113.6 kJ.mol^{-1}). Therefore, the mechanical energy afforded by the fully twisted system **W1-3** can be calculated to be 16.9 kJ.mol^{-1}, which represents the work the whirligig can effectively deliver in three half rotations. It is also apparent that it is within the last half rotation during UV irradiation that most of the energy is stored in the system. This latter energy allows us to state that the molecular motor can, at least, produce 13.2 kJ.mol^{-1} of effective work in a single half rotation to be able to overcome this thermal barrier. It should also be noted that the energy stored in the whirligig must be slightly higher than this value, because some is lost by dissipation and does not produce work during the reverse rotation process. It is, however, a very interesting lower estimate that is determined here as it shows the useful energy stored mechanically. In addition, even if the work delivered during the photoisomerization process could be, in principle, higher than this value, due to the absence of microreversibility between the forward and backward reactions, the thermal relaxation becomes a limiting factor because the ratchet mechanism (here involving the thermal *E*/*Z* isomerization of the double bond) cannot withstand a higher force. We present the overall picture of our whirligig approach with quantitative data in Figure 6. Knowing the value of the work produced, we determined the torque ~ 7 pN.nm) produced by a single whirligig **W1-3** (see SI section S7). Finally, by averaging the distances between the axle of the rotary motor with the atomic positions linked to the polymer chains (lever arm), we calculated an applied force of ~ 20 pN. As a reference, the torque produced by ATP synthase is evaluated in the literature at 40 pN.nm.[47] This experimental value of about 7 pN.nm determined for light triggered rotary motor is therefore very encouraging for their implementation in a number of applications.

CONCLUSION

By revisiting our original design of the figure-of-eight molecular motor / polymer conjugates,[40] we found structural conditions in which the system can both twist through the excited state under UV irradiation, and untwist fully at the ground state by reversing the directionality of the motor rotation. This observation should be kept in mind as a contributing (sometime limiting) factor when designing future systems using entanglements in single molecules[40,41,48] or in polymer networks such as gels.[35] Further, this exciting clockwise/anticlockwise inversion within

the molecular whirligig represents a new possibility to reset molecular motors pushed far from equilibrium through a dissipative pathway. Such cycles to store (by the excited state) and release (by the ground state) elastic energy may also be used to make these motors useful. Indeed, our observations demonstrate that the energy stored in the strained entanglements can be effective enough to produce a mechanical work which is sufficient to perform chemical transformations passing through high transition states (*i.e. E*/*Z* isomerization of a double bond), and thus opening new possibilities for mechanochemistry and catalysis in general. Moreover, our whirligig approach demonstrates the control of a function (*i.e.* strongly enhanced fluorescence by a motorized induced emission) which is modulated by this dissipative out-of-equilibrium pathway. Last but not least, the whirligig device turned out to be an unexpected platform of choice to quantitatively measure a lower estimate of the mechanical work, the torque and the force that can be reached with such light-triggered rotary motors. These questions were pending for a long time in the molecular machine community, and are now answered experimentally.

ASSOCIATED CONTENT

Supporting Information. Synthetic protocols and characterization of organic compounds, corresponding ^{1}H and ^{13} NMR spectra as well as HRMS spectra. Supplementary data on UV-Vis, CD, and fluorescence spectroscopies, as well as gel permeation chromatography are given in addition on the detailed analyses of the backward rotation kinetics. This material is available free of charge via the Internet at http://pubs.acs.org.

AUTHOR INFORMATION

Corresponding Author

* giuseppone@unistra.fr

ACKNOWLEDGMENT

The authors wish to acknowledge the LabEx CSC at the University of Strasbourg, and the Chinese Scholarship Council for a fellowship to CG. We also thank the "Plateforme de caractérisation des polymers" from the Institut Charles Sadron, Dr. Jean-Marc Strub, and Dr. Gilles Ulrich for GPC, HRMS experiments, and the measurement of fluorescence quantum yields respectively. We thank Odile Gavat for helping with the purification of some of the described compounds and their isomers. We are much grateful to Sir Fraser Stoddart who brought to our attention some years ago the term and principle of the macroscopic whirligig crafts during a lunch at a Gordon Research Conference. We also thank Jean-Pierre Sauvage and Anne-Sophie Duwez for discussions.

REFERENCES

(1) Balzani, V.; Credi, A.; Venturi, M. *Molecular Devices and Machines: Concepts and Perspectives for the Nanoworld;* Wiley-VCH: Weinheim, Germany, 2008. https://doi.org/10.1002/9783527621682.

(2) Sauvage, J.-P. From Chemical Topology to Molecular Machines (Nobel Lecture). *Angew. Chem. Int. Ed.* **2017**, *56* (37), 11080–11093. https://doi.org/10.1002/anie.201702992.

(3) Stoddart, J. F. Mechanically Interlocked Molecules (MIMs)-Molecular Shuttles, Switches, and Machines (Nobel Lecture). *Angew. Chem. Int. Ed.* **2017**, *56* (37), 11094–11125. https://doi.org/10.1002/anie.201703216.

(4) Feringa, B. L. The Art of Building Small: From Molecular Switches to Motors (Nobel Lecture). *Angew. Chem. Int. Ed.* **2017**, *56* (37), 11060–11078. https://doi.org/10.1002/anie.201702979.

(5) Bruns, C. J.; Stoddart, J. F. *The Nature of the Mechanical Bond*; John Wiley & Sons, Inc.: Hoboken, NJ, USA, 2016. https://doi.org/10.1002/9781119044123.

(6) Kassem, S.; van Leeuwen, T.; Lubbe, A. S.; Wilson, M. R.; Feringa, B. L.; Leigh, D. A. Artificial Molecular Motors. *Chem. Soc. Rev.* **2017**, *46* (9), 2592–2621. https://doi.org/10.1039/C7CS00245A.

(7) Lancia, F.; Ryabchun, A.; Katsonis, N. Life-like Motion Driven by Artificial Molecular Machines. *Nat. Rev. Chem.* **2019**, *3* (9), 536–551. https://doi.org/10.1038/s41570-019-0122-2.

(8) Zhang, L.; Marcos, V.; Leigh, D. A. Molecular Machines with Bio-Inspired Mechanisms. *Proc. Natl. Acad. Sci.* **2018**, *115* (38), 9397–9404. https://doi.org/10.1073/pnas.1712788115.

(9) Perrot, A.; Moulin, E.; Giuseppone, N. Extraction of Mechanical Work from Stimuli-Responsive Molecular Systems and Materials. *Trends Chem.* **2021**, *3* (11), 926–942. https://doi.org/10.1016/j.trechm.2021.08.007.

(10) Badjic, J. D.; Balzani, V.; Credi, A.; Silvi, S.; Stoddart, J. F. A Molecular Elevator. *Science* **2004**, *303* (5665), 1845–1849. https://doi.org/10.1126/science.1094791.

(11) Badjic, J. D.; Ronconi, C. M.; Stoddart, J. F.; Balzani, V.; Silvi, S.; Credi, A. Operating Molecular Elevators. *J. Am. Chem. Soc.* **2006**, *128* (5), 1489–1499. https://doi.org/10.1021/ja0543954.

(12) Kudernac, T.; Ruangsupapichat, N.; Parschau, M.; Macia, B.; Katsonis, N.; Harutyunyan, S. R.; Ernst, K.-H.; Feringa, B. L. Electrically Driven Directional Motion of a Four-Wheeled Molecule on a Metal Surface. *Nature* **2011**, *479* (7372), 208–211. https://doi.org/10.1038/nature10587

(13) Saywell, A.; Bakker, A.; Mielke, J.; Kumagai, T.; Wolf, M.; García-López, V.; Chiang, P.-T.; Tour, J. M.; Grill, L. Light-Induced Translation of Motorized Molecules on a Surface. *ACS Nano* **2016**, *10* (12), 10945–10952. https://doi.org/10.1021/acsnano.6b05650.

(14) Qiu, Y.; Feng, Y.; Guo, Q.-H.; Astumian, R. D.; Stoddart, J. F. Pumps through the Ages. *Chem* **2020**, *6* (8), 1952–1977. https://doi.org/10.1016/j.chempr.2020.07.009.

(15) Corra, S.; Casimiro, L.; Baroncini, M.; Groppi, J.; La Rosa, M.; Tranfić Bakić, M.; Silvi, S.; Credi, A. Artificial Supramolecular Pumps Powered by Light. *Chem. – A Eur. J.* **2021**, *27* (43), 11076–11083. https://doi.org/10.1002/chem.202101163.

(16) Feng, L.; Qiu, Y.; Guo, Q.-H.; Chen, Z.; Seale, J. S. W.; He, K.; Wu, H.; Feng, Y.; Farha, O. K.; Astumian, R. D.; et al. Active Mechanisorption Driven by Pumping Cassettes. *Science* **2021**, *374* (6572), 1215–1221. https://doi.org/10.1126/science.abk1391.

(17) Chen, S.; Wang, Y.; Nie, T.; Bao, C.; Wang, C.; Xu, T.; Lin, Q.; Qu, D.-H.; Gong, X.; Yang, Y.; et al. An Artificial Molecular Shuttle Operates in Lipid Bilayers for Ion Transport. *J. Am. Chem. Soc.* **2018**, *140* (51), 17992–17998. https://doi.org/10.1021/jacs.8b09580.

(18) Wang, W.-Z.; Huang, L.-B.; Zheng, S.-P.; Moulin, E.; Gavat, O.; Barboiu, M.; Giuseppone, N. Light-Driven Molecular Motors Boost the Selective Transport of Alkali Metal Ions through Phospholipid Bilayers. *J. Am. Chem. Soc.* **2021**, *143* (38), 15653–15660. https://doi.org/10.1021/jacs.1c05750.

(19) Kassem, S.; Lee, A. T. L.; Leigh, D. A.; Marcos, V.; Palmer, L. I.; Pisano, S. Stereodivergent Synthesis with a Programmable Molecular Machine. *Nature* **2017**, *549*

(7672), 374–378. https://doi.org/10.1038/nature23677.

(20) Lewandowski, B.; De Bo, G.; Ward, J. W.; Papmeyer, M.; Kuschel, S.; Aldegunde, M. J.; Gramlich, P. M. E.; Heckmann, D.; Goldup, S. M.; D'Souza, D. M.; et al. Sequence-Specific Peptide Synthesis by an Artificial Small-Molecule Machine. *Science* **2013**, *339* (6116), 189–193. https://doi.org/10.1126/science.1229753.

(21) Jiménez, M. C.; Dietrich-Buchecker, C.; Sauvage, J.-P. Towards Synthetic Molecular Muscles: Contraction and Stretching of a Linear Rotaxane Dimer. *Angew. Chem. Int. Ed.* **2000**, *39* (18), 3284–3287. https://doi.org/10.1002/1521-3773(20000915)39:18<3284::AID-ANIE3284>3.0.CO;2-7.

(22) Bruns, C. J.; Stoddart, J. F. Rotaxane-Based Molecular Muscles. *Acc. Chem. Res.* **2014**, *47* (7), 2186–2199. https://doi.org/10.1021/ar500138u.

(23) Goujon, A.; Moulin, E.; Fuks, G.; Giuseppone, N. [C2]Daisy Chain Rotaxanes as Molecular Muscles. *CCS Chem.* **2019**, *1*, 83–96. https://doi.org/10.31635/ccschem.019.20180023.

(24) Zheng, Y.; Han, M. K. L.; Zhao, R.; Blass, J.; Zhang, J.; Zhou, D. W.; Colard-Itté, J.-R.; Dattler, D.; Çolak, A.; Hoth, M.; et al. Optoregulated Force Application to Cellular Receptors Using Molecular Motors. *Nat. Commun.* **2021**, *12* (1), 3580. https://doi.org/10.1038/s41467-021-23815-4.

(25) von Delius, M.; Geertsema, E. M.; Leigh, D. A. A Synthetic Small Molecule That Can Walk down a Track. *Nat. Chem.* **2010**, *2* (2), 96–101. https://doi.org/10.1038/nchem.481.

(26) Škugor, M.; Valero, J.; Murayama, K.; Centola, M.; Asanuma, H.; Famulok, M. Orthogonally Photocontrolled Non-Autonomous DNA Walker. *Angew. Chem. Int. Ed.* **2019**, *58* (21), 6948–6951. https://doi.org/10.1002/anie.201901272.

(27) Cheng, C.; McGonigal, P. R.; Stoddart, J. F.; Astumian, R. D. Design and Synthesis of Nonequilibrium Systems. *ACS Nano* **2015**, *9* (9), 8672–8688. https://doi.org/10.1021/acsnano.5b03809.

(28) Giuseppone, N., Walther, A., Eds.; *Out-of-Equilibrium (Supra)Molecular Systems and Materials*; Wiley-VCH: Weinheim, Germany, 2021. https://www.doi.org/10.1002/9783527821990.

(29) Baroncini, M.; Silvi, S.; Credi, A. Photo- and Redox-Driven Artificial Molecular Motors. *Chem. Rev.* **2020**, *120* (1), 200–268. https://doi.org/10.1021/acs.chemrev.9b00291.

(30) Pezzato, C.; Cheng, C.; Stoddart, J. F.; Astumian, R. D. Mastering the Non-Equilibrium Assembly and Operation of Molecular Machines. *Chem. Soc. Rev.* **2017**, *46* (18), 5491–5507. https://doi.org/10.1039/C7CS00068E.

(31) Moulin, E.; Faour, L.; Carmona-Vargas, C. C.; Giuseppone, N. From Molecular Machines to Stimuli-Responsive Materials. *Adv. Mater.* **2020**, *32* (20), 1906036. https://doi.org/10.1002/adma.201906036.

(32) Aprahamian, I. The Future of Molecular Machines. *ACS Cent. Sci.* **2020**, *6* (3), 347–358. https://doi.org/10.1021/acscentsci.0c00064.

(33) Shi, Z.-T.; Zhang, Q.; Tian, H.; Qu, D.-H. Driving Smart Molecular Systems by Artificial Molecular Machines. *Adv. Intell. Syst.* **2020**, *2* (5), 1900169. https://doi.org/10.1002/aisy.201900169.

(34) Dattler, D.; Fuks, G.; Heiser, J.; Moulin, E.; Perrot, A.; Yao, X.; Giuseppone, N. Design of Collective Motions from Synthetic Molecular Switches, Rotors, and Motors. *Chem. Rev.* **2020**, *120* (1), 310–433. https://doi.org/10.1021/acs.chemrev.9b00288.

(35) Foy, J. T.; Li, Q.; Goujon, A.; Colard-Itté, J.-R.; Fuks, G.; Moulin, E.; Schiffmann, O.; Dattler, D.; Funeriu, D. P.; Giuseppone, N. Dual-Light Control of Nanomachines That Integrate Motor and Modulator Subunits. *Nat. Nanotechnol.* **2017**, *12* (6), 540–545. https://doi.org/10.1038/nnano.2017.28.

(36) Chen, J.; Leung, F. K.-C.; Stuart, M. C. A.; Kajitani, T.; Fukushima, T.; van der Giessen, E.; Feringa, B. L. Artificial Muscle-like Function from Hierarchical Supramolecular Assembly of Photoresponsive Molecular Motors. *Nat. Chem.* **2018**, *10* (2), 132–138. https://doi.org/10.1038/nchem.2887.

(37) Han, G. G. D.; Li, H.; Grossman, J. C. Optically-Controlled Long-Term Storage and Release of Thermal Energy in Phase-Change Materials. *Nat. Commun.* **2017**, *8* (1), 1446. https://doi.org/10.1038/s41467-017-01608-y.

(38) Mansø, M.; Petersen, A. U.; Wang, Z.; Erhart, P.; Nielsen, M. B.; Moth-Poulsen, K. Molecular Solar Thermal Energy Storage in Photoswitch Oligomers Increases Energy Densities and Storage Times. *Nat. Commun.* **2018**, *9* (1), 1945. https://doi.org/10.1038/s41467-018-04230-8.

(39) Bhamla, M. S.; Benson, B.; Chai, C.; Katsikis, G.; Johri, A.; Prakash, M. Hand-Powered Ultralow-Cost Paper Centrifuge. *Nat. Biomed. Eng.* **2017**, *1* (1), 0009. https://doi.org/10.1038/s41551-016-0009.

(40) Li, Q.; Fuks, G.; Moulin, E.; Maaloum, M.; Rawiso, M.; Kulic, I.; Foy, J. T.; Giuseppone, N. Macroscopic Contraction of a Gel Induced by the Integrated Motion of Light-Driven Molecular Motors. *Nat. Nanotechnol.* **2015**, *10* (1), 161–165. https://doi.org/10.1038/nnano.2014.315.

(41) Kathan, M.; Crespi, S.; Thiel, N. O.; Stares, D. L.; Morsa, D.; de Boer, J.; Pacella, G.; van den Enk, T.; Kobauri, P.; Portale, G.; Schalley, C. A.; Feringa, B. L. A Light-Fuelled Nanoratchet Shifts a Coupled Chemical Equilibrium. *Nat. Nanotechnol.* **2021**, *17*, 159–165. https://doi.org/10.1038/s41565-021-01021-z.

(42) Although we mention that the figure-of-eight whirligig presents a different number of crossings within its various **W1-X** isomers, one can change this number from one isomer to another one by rotation the central double of the motor. This occurs without breaking the topological links between the atoms, and therefore, the entire **W1-X** family displays the same topology from a strict mathematical point of view. The immediate consequence is that different **W1-X** cannot be considered as topological isomers or as different molecular knots. For excellent references on molecular topology, see: Sauvage, J. -P., Dietrich-Buchecker, C., Eds.; *Molecular Catenanes, Rotaxanes and Knots*; Wiley-VCH: Weinheim, Germany, 1999. https://doi.org/10.1002/9783527613724, and next reference.

(43) Fielden, S. D. P.; Leigh, D. A.; Woltering, S. L. Molecular Knots. *Angew. Chem. Int. Ed.* **2017**, *56* (37), 11166–11194. https://doi.org/10.1002/anie.201702531.

(44) Luo, J.; Xie, Z.; Lam, J. W. Y.; Cheng, L.; Chen, H.; Qiu, C.; Kwok, H. S.; Zhan, X.; Liu, Y.; Zhu, D.; et al. Aggregation-Induced Emission of 1-Methyl-1,2,3,4,5-Pentaphenylsilole. *Chem. Commun.* **2001**, No. 18, 1740–1741. https://doi.org/10.1039/B105159H.

(45) Mei, J.; Leung, N. L. C.; Kwok, R. T. K.; Lam, J. W. Y.; Tang, B. Z. Aggregation-Induced Emission: Together We Shine, United We Soar! *Chem. Rev.* **2015**, *115* (21), 11718–11940. https://doi.org/10.1021/acs.chemrev.5b00263.

(46) Hong, Y.; Lam, J. W. Y.; Tang, B. Z. Aggregation-Induced Emission. *Chem. Soc. Rev.* **2011**, *40* (11), 5361–

5388. https://doi.org/10.1039/c1cs15113d.
(47) Kinosita, K.; Yasuda, R.; Noji, H.; Adachi, K. A Rotary Molecular Motor That Can Work at near 100% Efficiency. *Philos. Trans. R. Soc. London. Ser. B Biol. Sci.* **2000**, *355* (1396), 473–489. https://doi.org/10.1098/rstb.2000.0589.
(48) In Ref 41, a partial reversibility of the system was also observed. However, probably because of the reversible chemical nature of their molecular design using imine bonds, the authors did not assign it to the back-rotation of the motor under mechanical strain, but rather to a non-defined uncatalyzed intramolecular reaction.

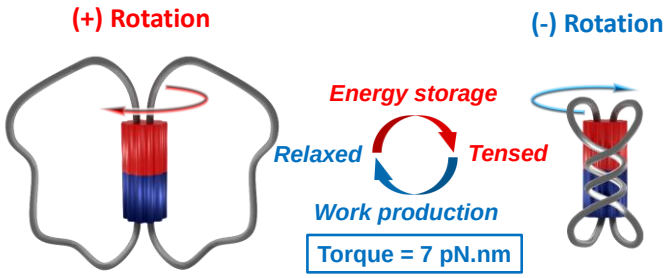
(+) Rotation
(-) Rotation
Energy storage
Relaxed
Tensed
Work production
Torque = 7 pN.nm